International Journal of Electrical, Electronic and Communication Sciences
ISSN: 2517-9438
Vol:3, No:4, 2009

Effects of Double Delta Doping on Millimeter and Sub-millimeter Wave Response of Two-Dimensional Hot Electrons in GaAs Nanostructures

N. Basanta Singh, Sanjoy Deb, G. P Mishra and Subir Kumar Sarkar

***Abstract*—**Carrier mobility has become the most important characteristic of high speed low dimensional devices. Due to development of very fast switching semiconductor devices, speed of computer and communication equipment has been increasing day by day and will continue to do so in future. As the response of any device depends on the carrier motion within the devices, extensive studies of carrier mobility in the devices has been established essential for the growth in the field of low dimensional devices. Small-signal ac transport of degenerate two-dimensional hot electrons in GaAs quantum wells is studied here incorporating deformation potential acoustic, polar optic and ionized impurity scattering in the framework of heated drifted Fermi-Dirac carrier distribution. Delta doping is considered in the calculations to investigate the effects of double delta doping on millimeter and sub-millimeter wave response of two dimensional hot electrons in GaAs nanostructures. The inclusion of delta doping is found to enhance considerably the two dimensional electron density which in turn improves the carrier mobility (both ac and dc) values in the GaAs quantum wells thereby providing scope of getting higher speed devices in future.

***Keywords*—**Carrier mobility, Delta doping, Hot carriers, Quantum wells.

I. Introduction

SINCE the beginning of the seventies, the microelectronics industry has followed Moore's law, doubling processing power every 18 months [1]. This performance increase has been achieved by increasing the speed and decreasing both the power consumption and size of devices and circuits. Continuous evolution in technology over the years has shrunk devices and systems so much that these dimensions are now less than a 1/10th of a micron. The term 'nanoelectronics' is therefore used instead of 'microelectronics'.

High-mobility two dimensional electron gas in modulation doped low dimensional structures such as quantum wells has attracted much attention because of the possibility of realization of high speed nano-devices. In such structure, mobility of the two-dimensional electron gas is enhanced considerably at low temperature by the so-called modulation doping technique [2]. This is due to spatial separation of electrons form donor impurities. The carrier mobility in GaAs quantum well (QW) is further enhanced by placing an undoped AlGaAs spacer layer between the doped AlGaAs and undoped GaAs layers [3]. The spacer layer increases the separation between the carriers and ionized donors thereby increasing the electron mobility because of less Coulomb interaction [4], [5]. The movement of charge carriers in a QW device depends on various factors like doping, carrier concentration, lattice temperature, applied field and carrier scattering etc. A lot of work is still going on to increase the mobility of carrier in a QW. There have been extensive studies in the nineties in the area of electronic state modulation followed by delta doping with an aim to enhance the carrier mobility [6], [7].

Polar-optical-phonon scattering is the most important scattering mechanism that limits electron mobility in a quantum well at room temperature [8], [9]. Therefore, for practical use of quantum well structures for very high speed application, it is desirable to suppress electron-phonon scattering which is dominant in modulation doped quantum well structures at temperature above 100K. Electronic-state modulation or wave function modulation is an attempt towards the achievement of such goal. In wave function modulation, thin barrier layers are inserted in the quantum well. Scattering strength in such type of modified heterostructure is reduced due to a change in the form factor for the interaction with phonon determined by the electron wave function along the direction perpendicular to the layer [10]. Several research works have suggested that the introduction of thin AlAs barriers in rectangular QWs leads to suppression of scattering by optical phonons, which in turn increases the electron mobility [10]-[13].

N. Basanta Singh is with the Department of Electronics and Communication Engineering, Manipur Institute of Technology, Imphal-795004, India (e-mail: basanta_n@rediffmail.com).

Sanjoy Deb is with the Dept. of Electronics and Telecommunication Engineering, Jadavpur University, Kolkata-32 India (e-mail: deb_sanjoy@yahoo.com).

G. P Mishra is with the Dept. of Electronics and Telecommunication Engineering, Jadavpur University, Kolkata-32 India (e-mail: gurumishra@rediffmail.com).

Subir Kumar Sarkar is with the Dept. of Electronics and Telecommunication Engineering, Jadavpur University, Kolkata-32 (corresponding author: +91-033-2410-7406; fax: +91-033-2414-6217; e-mail: su_sircir@yahoo.co.in).

Due to structural limitations such as 3D solubility limit of Si and Si impurity levels, the carrier density in the GaAs channel takes values less than $1x10^{12}$ cm^{-2} in single heterojunctions and somewhat higher but not exceeding 2 x 10^{12} cm^{-2} in quantum wells [14]. This carrier density limit in QW can be surpassed in delta doped heterostructures [15]. Delta doping is an important doping technique widely used in a number of semiconductor devices for extracting extraordinary features of the structures. Delta-doping, spike-doping and pulse-doping profiles are examples of extremely narrow but well defined doping profiles. Such profiles are required in semiconductor structures scaled to their practical and theoretical limits. As the spatial extent of the dopant distribution is much smaller than the de Broglie wavelength, the dopant distribution in delta doping can be represented by Dirac's delta function [16]. The delta doped quantum wells have the following advantages. The first advantage arises from those of the delta-doping technique, including higher mobility, greater electron density and uniform electron distribution [17]. The second advantage is the reduction of size of the quantum wells [17]. Since the spatial distribution of dopants is well controlled and confined to a single atomic layer, the size of the quantum well is reduced.

Delta doping allows us to localize impurities within one monolayer of the host semiconductor crystal [18] giving rise to quantization in a V shaped quantum well [19]. Very high electron concentrations exceeding 10^{13} cm^{-2} have been reported in delta doped GaAs [20].

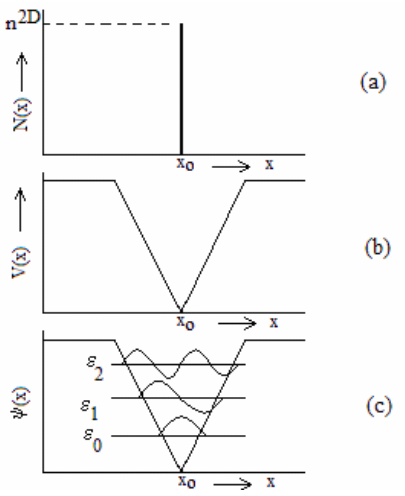

Fig. 1 Schematic diagrams of (a) the dopant distribution, (b) the V-shaped potential well and (c) the subband structure of a Si delta doped layer in GaAs.

The delta doping technique represents the ultimate technological limit of impurity profiles and this technique has resulted in a series of novel electronic and photonic devices [21], [22]. When a semiconductor is delta doped, the ionized donor atoms create a continuously positive sheet of charge which bends the conduction band to form a V-shaped potential well. The electrons remain close to their parent ionized donors as a result of the electrostatic attraction. When the dimension of the V-shaped potential well is comparable to the de Broglie wavelength of free electrons, the electron energies for motion perpendicular to the delta doped plane are quantized into a number of discrete bands and a quasi-two dimensional electron gas (2DEG) is formed in the V-shaped potential well. The dopant distribution, the potential well and the subband structure of a Si delta doped layer are shown in Figs. 1(a), (b) and (c).

The equations describing dopant concentration, the V-shaped potential well V(x) and energies ε_n are given in (1), (2) and (3), respectively [23].

$$N(x) = n^{2D}\delta(x - x_o) \tag{1}$$

$$V(x) = \begin{cases} -\frac{1}{2}\frac{en^{2D}}{k}(x - x_o) & for \quad x \le x_o \\ +\frac{1}{2}\frac{en^{2D}}{k}(x - x_o) & for \quad x \ge x_o \end{cases} \tag{2}$$

$$\varepsilon_n = \left[\frac{3\pi}{4}\left(n + \frac{1}{2}\right)\right]^{2/3}\left(\frac{e^2\hbar^2}{2m^*}\left(\frac{en^{2D}}{2k}\right)^2\right)^{1/3}, n = 0,1,... \tag{3}$$

Where n^{2D} is the donor density, e is the electronic charge, k is the dielectric constant, m* the effective mass and $\hbar$ is Planck's constant h divided by 2π.

It has been reported that the sheet density in delta doped structures is nearly doubled with respect to the densities obtained in modulation doped heterostructures [24], [25]. The growth of delta doped single heterojunction has been reported in [18]. Delta doped QW with 2D electron density of 4 x 10^{12} cm^{-2} in the GaAs channel has been reported in [25]. However, most the work in this area is concentrated in finding the carrier density and mobility in single sided delta doping heterostructures and quantum wells. All these have motivated us to study the effects of double sided delta doping on the carrier concentration and the small-signal mobility of the two dimensional hot electrons in a quantum well of GaAs/AlGaAs.

In the present work, we investigate the two dimensional electron densities confined in the quantum wells in delta doped GaAs/AlGaAs quantum well structures and show that the 2D electron density can be enhanced due to delta doping in the barrier AlGaAs layer. Our calculations are compared with data found in the literature. We also investigate the ac and dc mobility values in the delta doped GaAs quantum well in the framework of a heated drifted Fermi-Dirac distribution function and compared them with conventional homogeneously doped GaAs QW. The carrier scattering by longitudinal optic phonon, deformation potential acoustic phonons, remote and background-ionized impurities are incorporated in the present calculations. The dependence of ac and dc mobility values on the spacer width, channel width and doping density in the barrier layer are also investigated. The dependence of 3dB cut-off frequency on the spacer width, channel width and doping density in the barrier layer are also

studied.

II. THEORY

Let us consider the energy band diagrams of a delta doped heterostructure (δDH) of GaAs/AlGaAs and a conventional homogeneously doped heterostructure (HDH) of the same material. The energy band diagrams of such structures are shown in Figs. 2(a) and 2(b) [18]. All donor impurities are localized in a plane at a distance Ls from the GaAs/AlGaAs interface in δDH. This localization results in a V-shaped quantum well. The conduction band offset $\Delta\varepsilon_c$ can be written as

$$\Delta\varepsilon_c = \varepsilon_o + (\varepsilon_F - \varepsilon_o) + eFL_s - \varepsilon_o^1 - (\varepsilon_F - \varepsilon_o^1) \quad (4)$$

Where ε_o is the lowest subband energy in the well, $(\varepsilon_F-\varepsilon_o)$ is the degeneracy, $\Delta\varepsilon_c$ is the conduction band offset, ε_o^1 is the lowest energy state in the V-shaped quantum well and F is the electric field in the spacer layer. Assuming that there are no mobile carriers in the V-shaped well in AlGaAs i.e $(\varepsilon_F-\varepsilon_o^1)$ =0, (4) reduces to

$$\Delta\varepsilon_c = \varepsilon_o + (\varepsilon_F - \varepsilon_o) + eFL_s - \varepsilon_o^1 \quad (5)$$

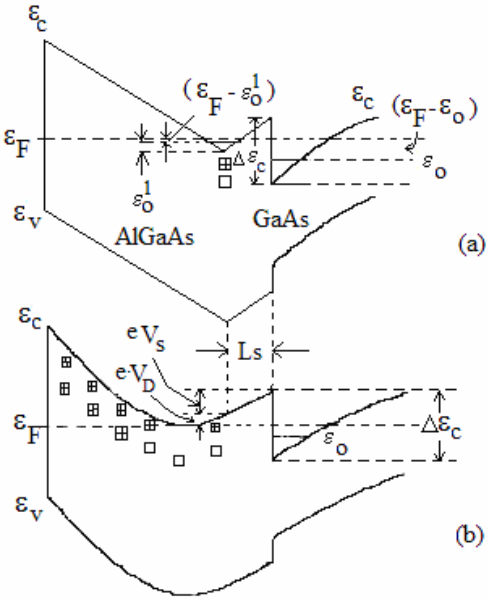

Fig. 2 Energy band diagram of a (a) delta doped heterostructure (δDH) and (b) a conventional homogeneously doped heterostructure (HDH).

For the homogeneously doped heterostructure, $\Delta\varepsilon_c$ can be written as

$$\Delta\varepsilon_c = \varepsilon_o + (\varepsilon_F - \varepsilon_o) + eFL_s + eV_D \quad (6)$$

Where, V_D is the potential drop in the deletion region. It is clear from (5) and (6) that in δDH there is no term for potential drop in the depletion region. This is due to localization of donor impurities in the delta doped AlGaAs. Secondly, the ε_o^1 adds up to the barrier height $\Delta\varepsilon_c$, thereby enhancing the effective conduction band discontinuity as compared to the HDH. The energy terms of (5) and (6) can be replaced by the following equations which are taken from [18] and the two dimensional electron gas concentrations in the quantum wells can be calculated.

$$\varepsilon_n = \frac{1}{2}(n+1)^{2/3}\left(e^2 2\pi\hbar n_{2D}/k_1\sqrt{m^*}\right)^{2/3}, n=0,1,\ldots \quad (7)$$

$$\varepsilon_F - \varepsilon_o = K_B TIn\left[\exp\left(n_{2D}\pi\hbar^2/K_B Tm^*\right)-1\right] \quad (8)$$

$$\Delta\varepsilon_c = 0.66\Delta\varepsilon_g \quad (9)$$

$$F = (e/k_2)n_{2D} \quad (10)$$

$$\varepsilon_n^1 = 2^{-7/3}(n+1)^{2/3}\left(2e^2\pi\hbar n^{2D}/k_2\sqrt{m^*}\right)^{2/3} \quad (11)$$

$$eV_D = e^2 n_{2D}^2/2k_2 n_D \quad (12)$$

In the above expressions, k_1 and k_2 are the dielectric constants in the well and barrier, K_B is the Boltzmann's constant, T is the temperature in Kelvin, $\Delta\varepsilon_g$ is the change in band gap, n_{2D} is the carrier concentration in the well, n^{2D} and n_D are the donor densities for δDH and HDH respectively.

Now, let us consider a GaAs/AlGaAs quantum well of width Lx. The AlGaAs barriers are symmetrically delta-doped at a distance Ls from the quantum well. A schematic diagram and a simplified energy band diagram of the delta doped GaAs quantum well is shown in Figs. 4 and 5. The total areal electron density in a delta doped QW well is known and is equal to the introduced doping density [15]. From the value of doping density and imposing charge neutrality, the value of total areal electron density is given by [15].

$$N = -\frac{1}{e}\int_{-\infty}^{+\infty}\rho_e(x)dx = 2n^{2D} \quad (13)$$

Where

$$\rho_e(x) = -e\sum_{jk} f(\varepsilon_f - \varepsilon_n(k))|\psi_{nk}(r)|^2$$

is the local electron density, n^{2D} is the doping density on each side and ε_f is the Fermi energy which is self consistently determined. The electron density can also be calculated from the energy balance equation [18]. The electron density in the QW due to single sided doping is a little more than one-half the values for the corresponding double sided doping [26]. Quantum size effects in Quantum well prevent the electron density from being exactly one half the electron density N_S of the double sided QW.

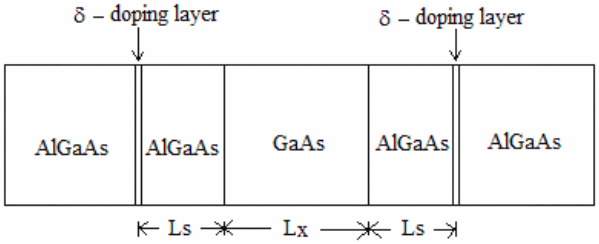

Fig. 3 A Schematic diagram of a delta doped GaAs/AlGaAs Quntum well

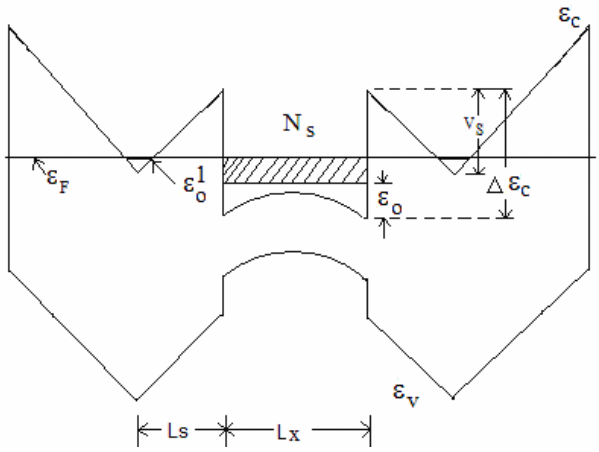

Fig. 4. A simplified Energy band diagram of a delta doped GaAs/AlGaAs Quantum well

In our proposed model, Ns is calculated using (14). Detailed derivation of N_S is depicted in the appendix.

$$N_S = \frac{\left(\Delta\varepsilon_C - \frac{h^2}{8m^*L_X^2} + 2^{-7/3}\left(e^2hn^{2D}/k_2\sqrt{m^*}\right)^{2/3}\right)}{\left(\frac{e^2L_X}{8k_1}\left(1+\frac{4}{\pi^2}\right) - \frac{e^2L_X}{24k_1}\left(1-\frac{3}{\pi^2}\right) + \frac{\pi\hbar^2}{m^*} + \frac{e^2}{2k_2}L_s\right)} \quad (14)$$

Improved carrier concentration and reduced ionized impurity scattering in the QW establish a strong electron-electron interaction, favouring a heated drifted Fermi-Dirac distribution function for the carriers characterized by an electron temperature T_e, and a drifted crystal momentum p_d [27]-[29]. In the presence of an electric field F applied parallel to the heterojunction interface, the carrier distribution function $f(\vec{k})$ can be expressed as,

$$f(\vec{k}) = f_o(E) + \frac{\hbar\vec{p}_d\vec{k}}{m^*}\left(-\frac{\partial f_o}{\partial E}\right)\cos\gamma \quad (15)$$

where, $f_o(E)$ is the Fermi-Dirac distribution function for the carriers, $\vec{p}_d$ is the drift crystal momentum, ħ is Planck's constant divided by 2π, $\vec{k}$ is the two-dimensional wave vector of the carriers with energy E, m* is the electronic effective mass and γ is the angle between the applied electric field $\vec{F}$ and the two dimensional wave vector $\vec{k}$.

An electric field of magnitude F_1 and the angular frequency ω superimposed on a moderate dc bias field F_0 is assumed to act parallel to the heterojunction interface. The net field is thus given by:

$$F = F_o + F_1\sin\omega t \quad (16)$$

As the electron temperature and the drift momentum depend on the field and the scattering processes, they will also have similar components with the alternating ones generally differing in phase. Thus

$$T_e = T_o + T_{1r}\sin\omega t + T_{1i}\cos\omega t \quad (17)$$

$$p_d = p_o + p_{1r}\sin\omega t + p_{1i}\cos\omega t \quad (18)$$

Where, T_0 and p_0 are the steady state parts, T_{1r} and p_{1r} are real and T_{1i} and p_{1i} are imaginary parts of T_e, and p_d respectively.

The energy and momentum balance equations obeyed by the carrier are:

$$ep_dF/m^* + \langle dE/dt\rangle_{scat} = \frac{d\langle E\rangle}{dt} \quad (19)$$

and

$$eF + \langle dp/dt\rangle_{scat} = \frac{dp_d}{dt} \quad (20)$$

Where - $\langle dp/dt\rangle$ and - $\langle dE/dt\rangle$, represents, respectively, the average momentum and energy loss due to scatterings and $\langle E\rangle$ depicts the average energy of a carrier with charge e. In the present model the effects of delta doping is included in the energy and momentum loss calculations to give more accurate results

We insert (17) and (18) in (19) and (20), retain terms up to the linear in alternating components and equate the steady parts and the coefficients of sinωt and cosωt on the two sides of the resulting equations following the procedure adopted in [28]. For a given electric field F_o, we solve for p_o and T_o. The dc mobility μ_{dc} and ac mobility μ_{ac} are then expressed as:

$$\mu_{dc} = \frac{p_o}{m^*F_o} \quad (21)$$

$$\mu_{ac} = \frac{\sqrt{p_{1r}^2 + p_{1i}^2}}{m^*F_1} \quad (22)$$

The phase lag ϕ, the resulting alternating current lags behind the applied field is expressed as

$$\phi = \tan^{-1}\left(-\frac{p_{1i}}{p_{1r}}\right) \quad (23)$$

III. RESULTS AND DISCUSSION

Numerical calculations are performed for delta doped GaAs/$Al_xGa_{1-x}As$ with the parameters give in Table I.

TABLE I
PARAMETERS EMPLOYED IN THE PRESENT CALCULATION FOR GaAs

Parameters	Values
Electron effective mass m^*(Kg)	0.61033×10^{-31}
Longitudinal elastic constant,C_l(N.m^{-2})	14.03×10^{10}
Static dielectric constant, K_S	12.52
Optic dielectric constant, K_∞	10.82
LO phonon angular frequency ω_o (rad/s)	5.37×10^{13}
Lattice Constant a(Å)	3.2
Acoustic deformation potential, E_1(J)	17.6×10^{-11}
Background ionized impurity concentration, n_{bi} (m^{-3})	6.0×10^{21}
Longitudinal acoustic velocity, u_L (ms^{-1})	5.11×10^{3}

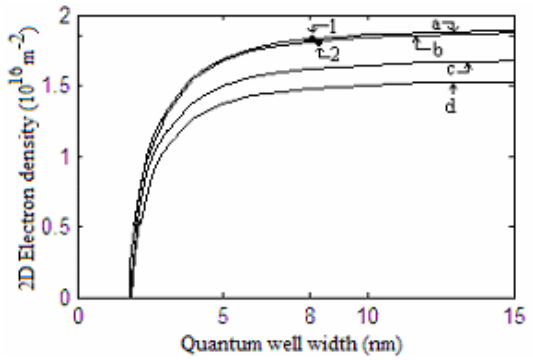

Fig. 5. Variation of 2D electron density N_S with quantum well width L_x with a doping density of 1 x10^{16} m^{-2} & x=0.3. The curves *a, b, c and d* shows the results with Ls values of 5 nm, 7 nm, 30nm & 50 nm respectively.

The variation of 2D electron density N_s with quantum well width L_x for different values of L_S for a doping density of 1x10^{16} m^{-2} is shown in Fig. 5. Curves *a,* b, c and *d* are for L_S values of 5nm, 7nm, 30nm, and 50nm respectively. The 2D electron density increases with increasing L_x and with decreasing L_S. Since larger spacer width implies larger potential decay V_S in the undoped layer, N_S decreases with increasing L_S. An increase of quantum well width with the same value of L_s results in an increase of 2D electron concentration. The dots (1 & 2) in the figure show results obtained in [15]. Our calculated results are found to agree with the previous theoretical work of [15]. The high concentration of two dimensional electron gas is due to the quantum size effect in the delta doped region and spatial localization of donor impurities [18]. The nature of variation can be explained in a manner similar to the work reported in [26].

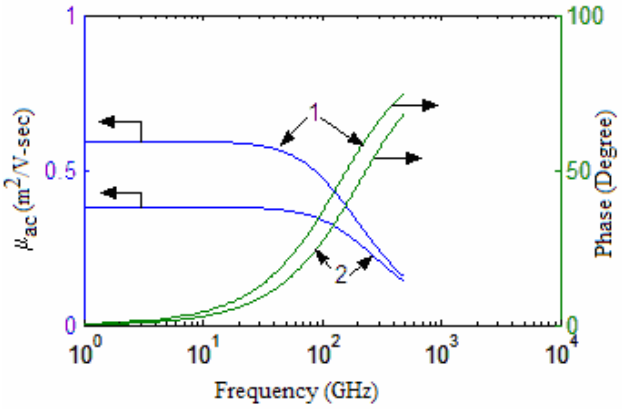

Fig. 6. Variation of μ_{ac} and phase with frequency of the applied field at 77K for L_x=10nm, L_s=5 nm, N_i=6x10^{21}m^{-3} and n^{2D}=1x10^{16} m^{-2}. The curves marked 1 and 2 represents the results for delta doped QW and conventional homogeneously doped QW.

Fig. 6 shows the variation of μ_{ac} and phase angle with frequency of the applied electric field for typical biasing field of 1x10^5V/m at 77K. The curves are obtained with the channel width Lx=10 nm, Ls=5 nm, a doping density of 1x10^{16} m^{-2} and a background ionized impurity concentration of 6x10^{21} m^{-3}. The ac mobility is found to be higher for the delta doped QW than the conventional homogeneously doped QW and it is due to more pronounced increase in ac mobility with enhanced carrier concentration in the former. The phase angle increase significantly beyond 30 GHz and is found to be higher for delta doping than conventional doping. The 3-dB cut-off frequency is 137GHz for delta doping and 199GHz for conventional doping thereby reflecting that delta doped QWs are frequency limited although their performance is better within the operating frequency limit. We have also got the similar nature of variation for μ_{ac} and phase angle at 300K with different magnitudes.

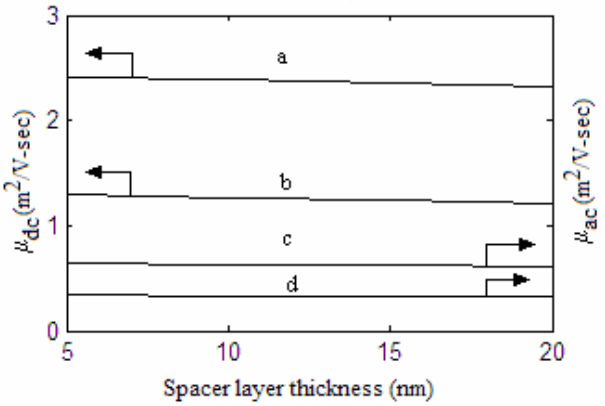

Fig. 7. Plot of μac and μdc with spacer layer thickness Ls for L_x=10 nm, N_i=6x10^{21}m^{-3} and n^{2D}=1x10^{16} m^{-2}. Curves *a* and *c* show the results for delta doped QW and curves *b* and *d* are for conventional homogeneously doped QW.

The variation of μ_{ac} and μ_{dc} with L_s for a lattice temperature of 77K is shown in Fig. 7. Both μ_{ac} and μ_{dc} decreases with increasing L_s due to increased potential decay in the undoped AlGaAs layer and reduction of the extent of carrier degeneracy as the influence of delta doping is decreased with the increase of L_s. The ac and dc mobility values are found to be higher for delta doped QW than the conventional doped QW due to pronounced carrier degeneracy and upward shift of Fermi-level [30].

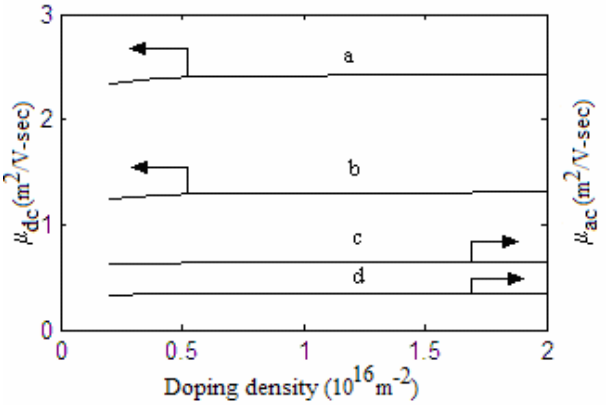

Fig. 8. Plot of μ_{ac} and μ_{dc} with doping density for L_x=10 nm, N_i=6x10^{21}m^{-3} and L_s= 5 nm. Curves *a - d,* have the same significance

as in Fig. 7.

The variation of μ_{ac} and μ_{dc} with doping density at 77K is given in Fig. 8. The curves *a* - *d* have the same significance as in Fig. 7. Both μ_{ac} and μ_{dc} increases with increasing doping density due to increased 2D electron density in the well. The weakening of scattering at higher 2D electron density due to enhanced screening and upward shift of Fermi level accounts for this behaviour [30]. The ac and dc mobility values are found to be higher for delta doped QW than the conventional doped QW due to enhanced 2D carrier concentration in the well and upward shift of Fermi-level [30].

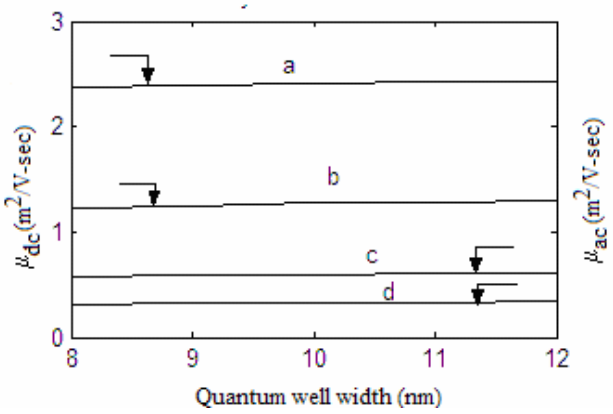

Fig. 9. Variation of μ_{ac} and μ_{dc} with L_x at 77K for L_s=5nm, N_i=6x10^{21}m^{-3} and n^{2D}=1x10^{16} m^{-2}. Curves *a* - *d,* have the same significance as in Fig. 7.

The variation of μ_{ac} and μ_{dc} with quantum well width L_x is shown in Fig. 9. μ_{ac} and μ_{dc} for both type of quantum wells increases with increasing L_x owing to reduced scattering for a higher channel width [30].

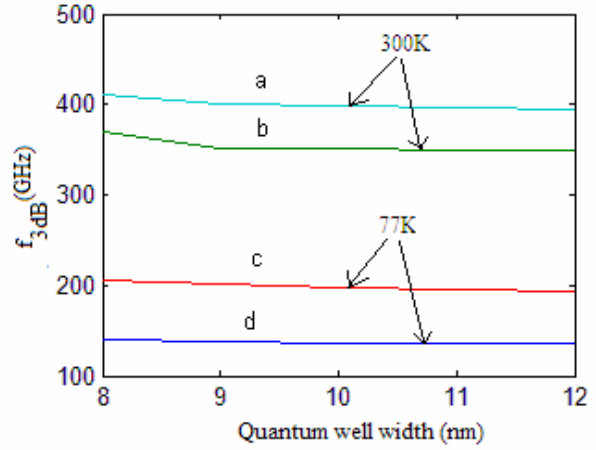

Fig. 10. Plot of f_{3dB} with L_x for 77K and 300K. Curves *a* and *c* are for conventional doping and b & d are for delta doping. The curves are plotted with L_s=5nm, N_i=6x10^{21}m^{-3} and n^{2D}=1x10^{16} m^{-2}).

Fig. 10 gives the plot of 3dB cut-off frequency f_{3dB} with channel width L_x for 77K and 300K. The curves *a* and *c* are for conventional doped QW. The curves *b* and *d* are for delta doped QW. The 3dB cut-off frequency is found to decrease with increasing L_x reflecting that the fall of μ_{ac} with frequency is sharper at a greater value of L_x [27]. The values of 3dB cut-off frequency is found to be higher at 300K that at 77K.

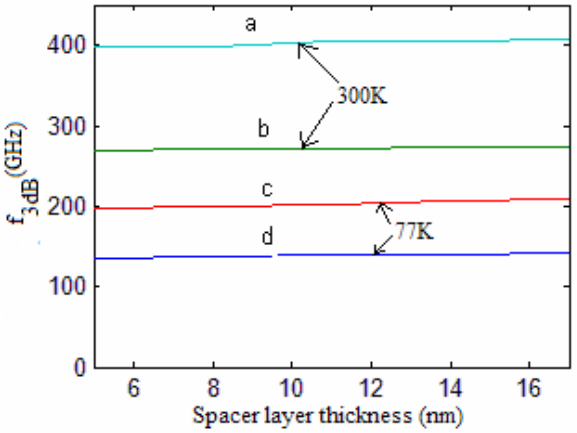

Fig. 11. Variation of f_{3dB} with Ls for 77K and 300K. Curves a - d have the same significance as in Fig.10 and are plotted with L_x=10 nm, N_i=6x10^{21}m^{-3} and n^{2D}=2x10^{16} m^{-2}.

Fig. 11 gives the plot of 3dB cut-off frequency with L_s for 77K and 300K. The curves *a* - *d* have the same significance as in Fig. 10. The 3dB cut-off frequency is found to increase with increasing L_s. This behaviour is explained with the reduced carrier degeneracy due to increase in L_s thereby reducing the influence of delta doping on surface states. The values of 3dB cut-off frequency f_{3dB} are higher at 300K than at 77K.

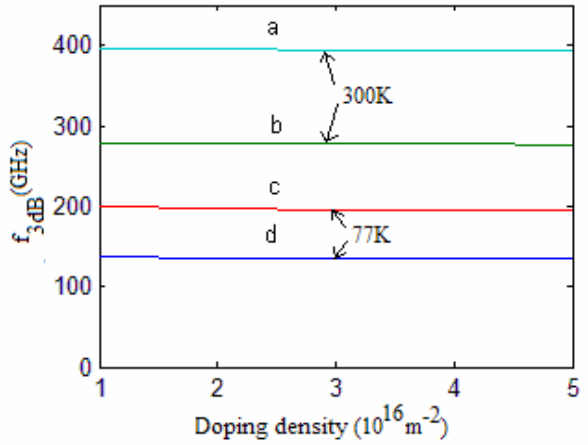

Fig. 12. Variation f_{3dB} with doping density for 77K and 300K (L_x= 10 nm, L_s=5 nm and N_i=6x10^{21}m^{-3}). Curves *a* - *d* have the same significance as in Fig.11.

Fig. 12 gives the plot of 3dB cut-off frequency f_{3dB} with doping density for 77K and 300K. The curves *a* - *d* have the same significance as in Fig. 11. The 3dB cut-off frequency is found to decrease with increasing doping density. This is because of the combined scattering mechanisms and increasing degeneracy of the carriers at higher 2D electron concentration [27]. The values of 3dB cut-off frequency are

higher at 300K than at 77K.

IV. Conclusion

In this work we have investigated the effects of delta doping on the carrier concentration, dc mobility, cut-off frequency and the small-signal mobility of the two dimensional electrons in a GaAs/AlGaAs QW. Our calculation shows the basic effect of 2D electron concentration and mobility enhancement in GaAs QW with delta doping in the barrier AlGaAs layer. The observed increase in 2D electron concentration of the GaAs well in delta doped structures is due to quantum-size effect. The dependencies of mobility (μ_{ac} & μ_{dc}) and 3dB cut-off frequency on various parameters are presented and explained with our model. The use of delta doping in the barrier layer leads to enhanced 2D electron density which in turn enhanced the carrier mobility in the QW thereby establishing the scope of getting high speed devices.

Appendix

Calculation of 2D electron density in a delta doped quantum well

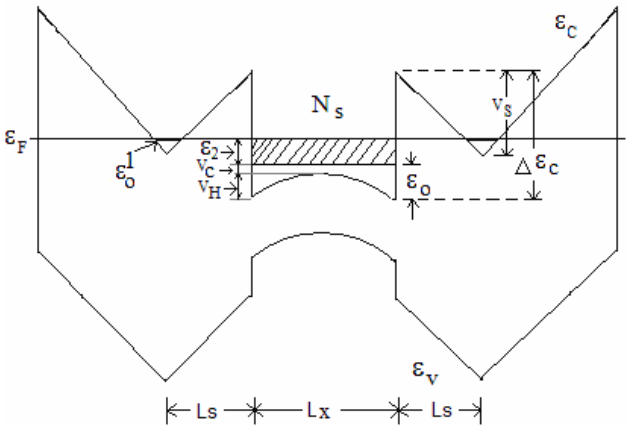

Assuming that only the lowest subband is occupied in the quantum well, the zero order approximation for the electronic wave function and potential in the QW are given by [26].

$$\psi_o(x) = (2/L_x)^{1/2} Cos\left(\frac{\pi x}{L_x}\right) \tag{A1}$$

and

$$V_o(x) = -\frac{e^2 N_S}{k_1 L_X}\left\{\left[1-\cos\left[\frac{2\pi x}{L_X}\right]\right]\frac{L_X^2}{4\pi^2}+\frac{x^2}{2}\right\} \tag{A2}$$

The energy balance equation can be written as

$$\Delta\varepsilon_c = V_H + V_C + \varepsilon_2 + V_S - \varepsilon_o^1 - \left(\varepsilon_F - \varepsilon_0^1\right) \tag{A3}$$

Assuming $(\varepsilon_F - \varepsilon_o^1) = 0$, (A3) reduces to

$$\Delta\varepsilon_c = V_H + V_C + \varepsilon_2 + V_S - \varepsilon_o^1 \tag{A4}$$

The value for confinement energy V_c from the first-order perturbation theory is

$$V_C = \frac{h^2}{8m^* L_x^2} - \frac{e^2 N_S L_x}{24k_1}\left(1-\frac{3}{\pi^2}\right) \tag{A5}$$

The values of the remaining terms are given below:

$$V_H = \frac{e^2 N_S L_x}{8k_1}\left(1+\frac{4}{\pi^2}\right) \tag{A6}$$

$$\varepsilon_2 = \frac{\pi\hbar^2}{m^*} N_S \tag{A7}$$

$$V_S = \frac{e^2 N_S}{2k_2} L_s \tag{A8}$$

$$\varepsilon_n^1 = 2^{-7/3}(n+1)^{2/3}\left(e^2 2\pi\hbar n^{2D}/k_2\sqrt{m^*}\right)^{2/3} \tag{A9}$$

$$\Delta\varepsilon_c = 0.66\Delta\varepsilon_g \tag{A10}$$

In the above expression k_1 and k_2 are the dielectric constants in GaAs and AlGaAs respectively, K_B is Boltzmann's constant, $\Delta\varepsilon_g$ is the change in band gap, N_S is the carrier concentration in the well and n^{2D} is the donor density.

Inserting the above values in [A4], we derived [A11]

$$\Delta\varepsilon_C = \frac{e^2 N_S L_X}{8k_1}\left(1+\frac{4}{\pi^2}\right)+\frac{h^2}{8m^* L_x^2}-\frac{e^2 N_S L_X}{24k_1}\left(1-\frac{3}{\pi^2}\right)+ \frac{\pi\hbar^2}{m^*}N_S+\frac{e^2 N_S}{2k_2}L_s-2^{-7/3}\left(e^2 hn^{2D}/k_2\sqrt{m^*}\right)^{2/3} \tag{A11}$$

$$N_S = \frac{\left(\Delta\varepsilon_C - \frac{h^2}{8m^* L_X^2}+2^{-7/3}\left(e^2 hn^{2D}/k_2\sqrt{m^*}\right)^{2/3}\right)}{\left(\frac{e^2 L_X}{8k_1}\left(1+\frac{4}{\pi^2}\right)-\frac{e^2 L_X}{24k_1}\left(1-\frac{3}{\pi^2}\right)+\frac{\pi\hbar^2}{m^*}+\frac{e^2}{2k_2}L_s\right)} \tag{A12}$$

References

[1] "Technology roadmap for nanoelectronics," Published by European Commission IST programme on Future and Emerging Technologies, Nov. 2000. Available: http://www.cordis.lu/ist/fetnid.htm.

[2] R. Dingle, H. L. Stormer, A. C. Gossard and W. Wiegmann, "Electron mobilities in modulation-doped semiconductor heterojunction superlattices," *Appl. Phys. Lett.,* vol. 33, no. 7, pp. 665-667, Oct. 1978.

[3] J. J. Harris, J A Pals and R Woltjer, "Electronic transport in low-dimensional structures," *Rep. Prog. Phys*., vol. 52, pp.1217-1266, Oct. 1989.

[4] C T Foxon, J J Harris, D Hilton, J Hewett and C Roberts, "Optimisation of (Al,Ga)As/GaAs two-dimensional electron gas structures for low carrier densities & ultra high mobilities at low temperature, "*Semicond. Sci. Technol.*, vol. 4, pp. 582-595, Apr. 1989.

[5] M. Heiblum, E. E. Mendez and F. Stern, "High mobility electron gas in selectively doped *n*:AlGaAs/GaAs heterojunctions," *Appl. Phys. Lett.,* vol. 44, no.11, pp. 1064-1066, Jun. 1984

[6] E. F. Schubert, "Delta doping of III-V compound semiconductor: Fundamental and device applications*, "J. Vac. Sci. Technol. A,* vol. 87, no. 3, pp. 2980-2996, May 1990

[7] Guo-Qiang Hai, Nelson Studart and F. M. Peeters, "Electron mobility in two coupled δ layers, " *Phys. Rev. B,* vol. 52, no. 15, pp.11273-11276, Oct. 1995

[8] P. J. Price, "Two-dimensional electron transport in semiconductor layers. I. Phonon scattering," *Ann. Phys*., vol. 133, pp. 217-239, May. 1981.

[9] T. Tsuchiya and T Ando, "Electron-phonon interaction in GaAs/AlAs superlattices," Phys. Rev. B, vol. 47, no. 12, pp. 7240-7252, Mar. 1993.

[10] T. Tsuchiya and T Ando, "Mobility enhancement in quantum wells by electronic-state modulation," *Phys. Rev. B,* vol. 48, no. 7, pp. 4599-4603, Aug. 1993

[11] Subir Kumar Sarkar, "Effects of wave function modulation on high-frequency carrier transport in quantum wells under high biasing field," *Indian J. Phys*., vol. 78, no. 7, pp. 535-538, 2004.
[12] X. T Zhu, H. Goronkin, G. N. Maracas, R. Droopad and M. Stroscio, " Electron mobility enhancement by confining optical phonons in GaAs/AlAs multiple quantum wells," *Appl. Phys. Lett*., vol. 60, no. 17**,** pp**.** 2141-2143, Apr. 1992.
[13] J. Pozela, V. Juciene , A. Namajunas and K. Pozela, "Electron mobility and subband population tuning by a phonon wall inserted in a semiconductor quantum well, "*J. Appl. Phys.,* vol. 81, no. 4, pp. 1775-1780, Feb. 1997.
[14] H. Harikawa, H. Sakaki and J. Yoshino, "Concentrations of electrons in selectively doped GaAlAs/GaAs heterojunction and its dependence on spacer layer thickness and gate electric field," *Appl. Phys. Lett*., vol. 45, no. 3, pp. 253-255, Aug. 1984.
[15] L. Chico, W Laskolski, R Perez-Alvarez and F Garcia Moliner, "On the theory of GaAs-based quantum wells with external δ-doping, *J. Phys.: Condens. Matters,* vol. 5, pp.9069-9076 Aug. 1993.
[16] H.J Gossmann and E.F. Schubert, "Delta doping in Silicone," *Solid State and Material Sc.,* vol. 18, no. 1, pp. 1-67, Jan. 1993
[17] Ikai Lo, Y. C. Chang, H. M. Weng, and J. C. Chiang, "Two-dimensional electron gas in δ-doped double quantum wells for photodetector application," *J. Appl. Phys*., vol. 81, no. 12, pp. 8112-8114, Jun. 1997.
[18] E. F Schubert, J. E. Cunningham, W.T Tsang and G.L. Timp, "Selectively δ-doped $Al_xGa_{1-x}As$/GaAs heterostructures with high two-dimensional electron-gas concentrations $n_{2DEG}>1.5x10^{12}$ cm^{-2} for field-effect transistors, "*Appl. Phys. Lett.,* vol. 51, no. 15, pp. 1170-1172 Oct. 1987
[19] E. F Schubert, A. Fischer and K. Ploog, "The delta doped field effect transistor (δFET), "*IEEE Trans. Electron Devices,* vol. 33, no. 5, pp. 625-632 May 1986.
[20] E. F Schubert, J. E. Cunningham, W.T Tsang, "Electron-mobility enhancement and electron-concentration enhancement in δ-doped n-GaAs at T=300K, " *Solid State Commun*., vol. 63, pp. 591-594, 1987
[21] E. F Schubert, J. E. Cunningham, and W.T Tsang, "Self-aligned enhancement-mode and depletion-mode GaAs field effect transistor employing the δ-doping technique," *Appl. Phys. Lett*., 49, no. 25, pp. 1729-1731, Dec. 1986.
[22] E. F Schubert, A. Fischer, Y. Horikoshi, and K. Ploog, "GaAs sawtooth superlattice laser emitting at wavelength λ>0.9μm," *Appl. Phys. Lett*., vol. 47, no. 3, pp. 219-221, Aug. 1985.
[23] H.J Gossmann and E.F. Schubert, "Delta doping in Silicone," *Solid State & Material Sc.,* vol. 18, no. 1, pp. 1-67, Jan. 1993.
[24] J. E. Cunningham, W.T. Tsang, G. Timp, E. F. Schubert, A. M. Chang and K. Owusu-Sekyer, " Quantum size effects in monolayer doped heterostructures," *Phys. Rev. B,* vol. 37,no. 8, pp. 4317-4320, Mar. 1988.
[25] T. Y Kuo, J. E Cunningham, E. F Schubert, W. T Tsang, T. H Chiu, R Ren and C. G Fonstad, " Selectively δ-doped quantum well transistor grown by gas source molecular beam epitaxy," *J. Appl. Phys*., vol. 64, no. 6, pp. 3324- 3327, Sept. 1988.
[26] V.M.S.Gomes,A.S. Chavas, J. R Leite and J.M.Worlock,"Self-consistent calculations of the two-dimensional electron density in modulation-doped superlattices*," Phys. Rev. B*, 35 (8), pp. 3984-3989, Mar. 1978.
[27] S. K. Sarkar,P. K. Ghosh and D. Chattopadhyay, "Calculations of high-frequency response of two-dimensional hot electrons in GaAs quantum wells," *J. Appl. Phys.,* vol. 78, no. 1, pp. 283-287, July 1995.
[28] S. K. Sarkar, "Multiple level optimization for high frequency ac mobility in GaAs quantum wells under hot-electron condition," *Comp. Mat. Sci.*, vol-29, pp. 243-249, 2004.
[29] S. K. Sarkar, A. Moi , C. Puttamadappa , A.K. Day and M.K. Naskar, "Application of genetic algorithm to determine the optimized system parameters of GaAs quantum wells for better high-frequency performance under hot electron condition," *Physica B*, vol. 325, pp.189-194, 2003.
[30] J. P. Leburton, "Size effects on polar optical phonon scattering of 1-D and 2-D electron gas in synthetic